Geophys. J. Int. (2006) **167,** 959–967 doi: 10.1111/j.1365-246X.2006.03152.x

FAST TRACK PAPER

Shear wave splitting changes associated with the 2001 volcanic eruption on Mt Etna

Francesca Bianco,[1] Luciano Scarfì,[2] Edoardo Del Pezzo[1] and Domenico Patanè[2]

[1] *Istituto Nazionale Geofisica e Vulcanologia, Osservatorio Vesuviano, Napoli, Italy. E-mail: bianco@ov.ingv.it*
[2] *Istituto Nazionale Geofisica e Vulcanologia Sez. Catania, Italy*

Accepted 2006 July 25. Received 2006 July 25; in original form 2005 April 13

SUMMARY

The time delays and polarizations of shear wave splitting above small earthquakes show variations before the 2001 July 17–August 9 2001 flank eruption on Mt Etna, Sicily. Normalized time delays, measured by singular value decomposition, show a systematic increase starting several days before the onset of the eruption. On several occasions before the eruption, the polarization directions of the shear waves at Station MNT, closest to the eruption, show 90°-flips where the faster and slower split shear waves exchange polarizations. The last 90°-flip being 5 days before the onset of the eruption. The time delays also exhibit a sudden decrease shortly before the start of the eruption suggesting the possible occurrence of a 'relaxation' phenomena, due to crack coalescence. This behaviour has many similarities to that observed before a number of earthquakes elsewhere.

Key words: cracked media, seismic anisotropy, shear wave splitting, volcanic activity, volcanic structure, wave propagation.

INTRODUCTION

Shear wave splitting is the elastic analogue of the well-known optical birefringence phenomenon. When a shear wave enters an anisotropic solid, it splits into two different quasi-shear waves with different velocities and approximately orthogonal polarizations (Crampin 1981). The two diagnostic properties are φ, the azimuthal polarization of the faster split shear wave in the horizontal plane, and δt, the time delay between the split shear waves, which we normalize by the hypocentral distance. Crampin *et al.* (1984) introduced the extensive-dilatancy anisotropy (EDA) hypothesis suggesting that the cause of the stress-aligned shear wave splitting observed throughout the crust is the distribution of fluid-saturated grain-boundary cracks and aligned pores in almost all rocks in the crust. Such fluid-saturated microcracks are highly compliant and are aligned by the stress field into typically parallel vertical orientations. The evolution of such fluid-saturated cracks under deformation can be calculated by the anisotropic poro-elasticity (APE) model of fluid-rock deformation, where the driving mechanism is fluid migration by flow or diffusion along pressure gradients between microcracks at different orientations to the stress-field (Zatsepin & Crampin 1997; Crampin & Zatsepin 1997).

APE modelling shows that fluid-saturated microcracks open, like hydraulic fractures, perpendicular to the direction of minimum compressional stress. Observations of shear wave splitting at the surface show near parallel polarizations striking in the direction of maximum horizontal stress (Crampin 1999).

Crampin (1999) shows that changes of aspect-ratio modify shear wave splitting time delays in Band-1 of the shear wave window. Band-1 is the double-leafed solid-angle with directions between 15° and 45° either side of the average plane of the parallel cracks in the shear wave window. Band-2, directions 15° either side of the crack plane, are sensitive principally to crack density, and field observations have not been observed to display distinctive variations (Volti & Crampin 2003a,b). (Note that the shear wave window can usually be extended to 45° to allow for the effects of low-velocity near-surface layers on incidence angles at the surface.)

In the present paper we deal with the experimental measure of the splitting parameters at Mt Etna volcano, in order to enlighten possible changes before the main eruptive phenomena occurred during the activity period of 2001.

The association of these changes with the occurrence of earthquakes and/or eruptions is still matter of debate, since experimental studies report either temporal changes of the splitting parameters related to the occurrence of several earthquakes, or no clear variations for some others. In particular, time delays in Band-1 have been observed to increase before some 15 earthquakes worldwide ranging in magnitude from M 1.7 to Ms 7.7 (Crampin *et al.* 1990, 1991; Gao *et al.* 1998; Volti & Crampin 2003b; Gao & Crampin 2004; Crampin & Gao 2005). In the framework of the APE modelling, the hypothesis is that the impending earthquake occurs when the crack distributions reach levels of fracture criticality, where the magnitude of the earthquake is proportional to the duration of the increase in time delays. Rapid variations of shear wave splitting have also been

observed after two moderate seismic events, $M = 4.2$ and $M = 4.4$ in Southern California (Li *et al.* 1994), and in an active experiment carried out in the KTB borehole in southeastern Germany after a fluid-injection-induced swarm of microearthquakes (Bokelmann & Harjes 2000; Tang *et al.* 2005). Teanby *et al.* (2004) showed evidences of temporal variations in shear wave splitting observed in microseismic data, interpreting their observations in term of stress-controlled cracks, suggesting that shear wave splitting is a viable probe to infer crustal stress changes in cracked rocks.

On the other hand, Liu *et al.* (2004) observed a lack of variations of the splitting parameters for the 1999 Chi Chi earthquake [Crampin & Gao (2005), commented this paper proposing a different interpretation of these data]. Peng & Ben-Zion (2005) interpreted the observed variations of the splitting parameters measured for the aftershocks of the Izmit and Dűzce (Turkey) earthquakes as mainly due to spatial variations of the ray paths due to the changing of the seismicity features. So, the issue of temporal changes in splitting before earthquakes appears to be highly controversial.

The results obtained for the observations related to changing in the volcanic activities seems to be more stable and promising. In volcanic areas, changes in shear wave splitting have been observed during the 1989 eruption at Mt Etna, Sicily (Bianco *et al.* 1998), before the eruption of Mount Ruapehu, New Zealand (Miller & Savage 2001; Gerst & Savage 2004); before the 1996 October eruption at Vatnajökull, Iceland (Volti & Crampin 2003b), and before the M 3.6 earthquake at Mt Vesuvius, 1999 October, the strongest since the end of the last 1944 eruption (Del Pezzo *et al.* 2004).

We measured the splitting parameters at Mt Etna for seismicity during the period 2001 January–December, spanning the July eruption. We report variations of both depth-normalized δt and φ several days before the start of the effusive phase. Our measures appear to be in agreement with APE modelling, and are similar to other observations before earthquakes obtained elsewhere, introducing the debate on the possibility that variations in shear wave splitting may be a new class of precursor for the impending eruptions at Mt Etna; however, we introduce also possible alternative explanations on our findings, in order to make a more complete discussion on the possible causes of the observed pattern.

DATA ANALYSIS AND RESULTS

Mt Etna experiences many eruptions and its almost persistent seismic activity makes it a natural laboratory for volcano-seismic studies. On 2001 July 17, a flank eruption began after 3 months of increasing seismic activity and fountaining lava at the SE Crater. On the night of 2001 July 12, an intense seismic swarm, of ∼2660 events located at south of the summit of Mt Etna, accompanied the opening of a NS surface fracture (inset, Fig. 1). The swarm continued into the early hours of July 18, and at 2:20 am lava was ejected from the southern tip of the fissure. This lateral eruption ended on 2001 August 9. For a detailed description of the seismicity related to the 2001 eruption, as well as for the details on the medium model, the location procedure and the accuracy of locations see Musumeci *et al.* (2004) and references therein (we just used a subset of their data referring to their locations).

The splitting parameter measurements were performed applying a rigorous selection of seismic records, according to the following criteria: (i) clear shear wave onsets with signal-to-noise ratios S/N > 6 and (ii) angles of incidence inside the shear wave window. We analysed selected data from two digital high-gain three-component seismic stations ESP and MNT (Fig. 1). Unfortunately, no data from other stations of the network passed our selection rules,

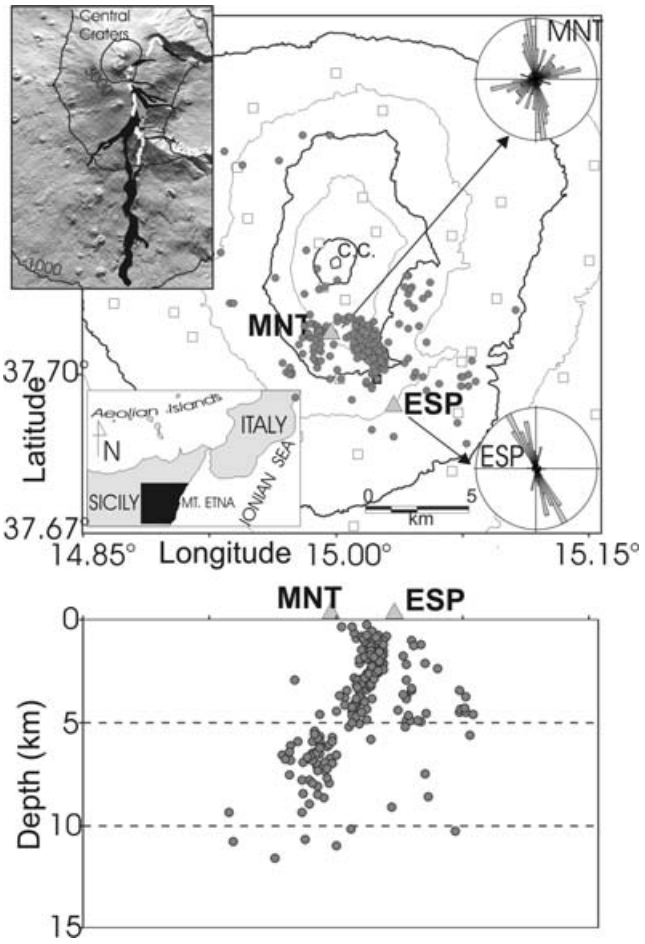

Figure 1. Epicentral map and hypocentral EW cross-section of the 134 earthquakes (grey dots) used in this study. The location of the seismic stations (open squares) of the INGV-CT permanent network is also shown. Grey triangles are the two 3C digital seismic stations MNT and ESP selected for our analysis. On the right, rose-diagrams show polarizations of φ at both stations for the entire analysed period. The map at top left, shows the surface fractures (in white) and the lava flows (in black) of the 2001 flank eruption.

so we have no other available waveforms. Our data set contains 134 earthquakes with magnitude $1.3 \leq M \leq 3.1$ and depths in the range 3–20 km, in the period 2001 January–December; all of them were recorded at station ESP, and 111 recorded at station MNT. Hypocentral distribution and location are shown in Fig. 1.

We measured the splitting parameter δt using the properties of the orthogonal transformations, as suggested by Shieh (1997). We consider the $n \times 3$ matrix **A**, whose columns contain the vertical and the two horizontal component seismograms, respectively $z(t)$, $x(t)$, and $y(t)$. The matrix **A** can be written as $\mathbf{A} = \mathbf{U}\,\mathbf{\Sigma}\,\mathbf{V}^{\mathrm{T}}$, where **U** is a $n \times n$ orthogonal matrix, $\mathbf{\Sigma}$ is $n \times 3$ diagonal matrix of eigenvalues, and **V** is a 3×3 orthogonal matrix. Using an orthogonal transformation singular-value decomposition (SVD) the components of the ground motion are decomposed into the fast $F(t)$, slow $S(t)$ and noise $N(t)$ components, according to the following:

$$\begin{aligned} F(t) &= \lambda_1 \cdot U(t,1), \\ S(t) &= \lambda_2 \cdot U(t,2), \\ N(t) &= \lambda_3 \cdot U(t,3); \end{aligned} \tag{1}$$

where $U(t,1)$, $U(t,2)$ and $U(t,3)$ are the first three columns of the **U** matrix. The measure of δt is obtained by cross-correlating $F(t)$ with

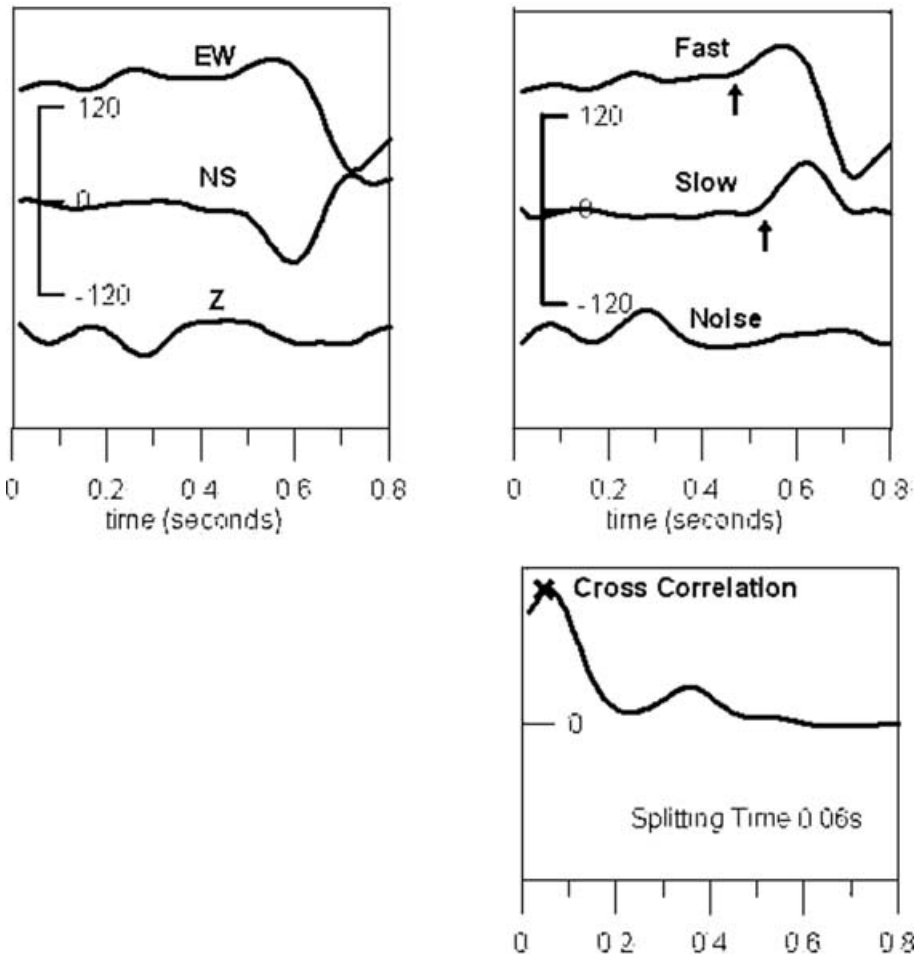

Figure 2. An example of the SVD procedure to determine δt values. The recorded 3C signal (top left) is decomposed into the fast, slow and noise components (top right). The cross-correlation function between the Fast and the Slow components is shown with an indication of the measured splitting δt.

$S(t)$ with the assumption that the noise was confined to $N(t)$. δt is then normalized to 1 km by dividing by the corresponding hypocentral distance D. We also performed a normalization to the traveltimes (Liu *et al.* 2005a) obtaining a compatible trend. An example of the seismic traces and of the corresponding traces obtained applying the SVD procedure is shown in Fig. 2. Note that all results are checked in particle-motion diagrams (hodograms) to avoid possible cycle skipping and other anomalous effects.

Crampin (1999) shows that time delays vary with the direction of propagation and behave differently in Band-1 and Band-2 directions.

Time delays in Band-1

We averaged the measures in nine-point moving averages of the normalized δt, in a three-point steps, for Band-1 ray paths for both ESP and MNT. Results are reported in Fig. 3(a). Note that Station MNT ceased to work on July 15 having been damaged by lava. The error bars in Fig. 3 correspond to the standard deviation:

$$\sigma_{\delta t} = \left(D^{-2}\sigma_{Td}^2 + D^{-4}\sigma_D^2 T_d^2\right)^{1/2}. \quad (2)$$

In formula (2) T_d is the measure obtained by cross-correlating $F(t)$ with $S(t)$ and we assume that the error associated with its estimate, σ_{Td} is of the order of three samples (0.02 s, Del Pezzo *et al.* 2004), and that the error associated with the hypocentral distance, σ_D, is of the order of 0.2 km.

At both stations, the normalized time delays in Band-1 show a similar pattern: a long-term increase that begins several days (about 70 d for the filtered signal) before the start of the effusive eruption (2001 July 17), and a short-term decrease starting 2 to 3 d before the eruption. These variations in δt are similar to those observed before impending earthquakes in several places elsewhere.

We carried out a t-test to show that the averages of the values before and after 70 days before the start of the effusive eruption are not different by chance. We averaged the T_n values in a time interval of 70 days before and after the turning point for the values in Band-1 at both stations (Fig. 3a), showing that the averages, in all the cases, are different at a 99 per cent confidence level.

Time delays in Band-2

For Station ESP, there were only three events with ray paths in Band-2 for the analysed period, and these are not plotted. For station MNT, the ray paths in Band-2 are mainly concentrated in the first 80 d of observations; after this period only two events with ray paths in Band-2 occurred on 2001 July and these are not shown in Fig. 3(a). The distribution of δt values in Band-2 at station MNT does not show any statistically significant variation.

Shear wave polarizations, φ

The splitting parameter φ was obtained by 3-D covariance matrix decomposition (Born & Wolf 1965) by estimating the eigenvector

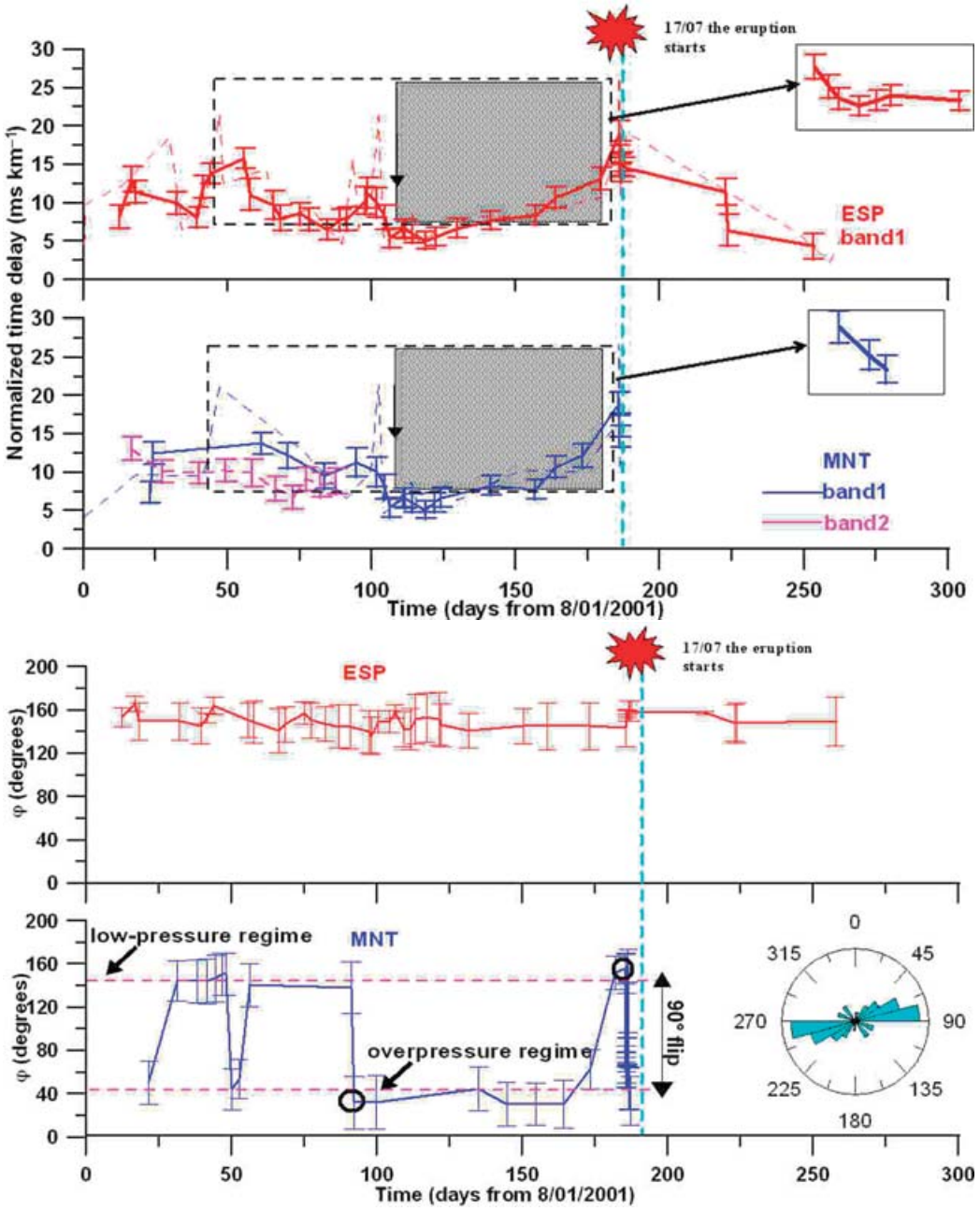

Figure 3. (a) Nine-point averages (in three-event steps) of normalized time delay δt (solid line) and the unfiltered behaviour (dashed line) for station ESP in upper diagram, and Station MNT in lower diagram. The dashed rectangle represents the window on which the t-test has been carried out, and the arrow inside the rectangle signs the location of the start of the increasing (the increasing zone is included in the shadow rectangle). In the lateral insets a zoom of the δt behaviour in the 3 days preceding the onset of the eruption are reported. (b) Nine-point moving averages (in three-event steps) of φ for stations ESP and MNT. The horizontal dashed lines in MNT are averages of the oscillation about 90° indicating 90°-flips. A rose-diagram for φ at MNT shows polarizations for the 5 days immediately preceding the eruption.

related to the largest eigenvalue in the horizontal plane. The rose-diagrams for the complete set of data (Fig. 1) show that the qS1 polarization directions strike approximately NNW–SSE at both ESP and MNT stations. The nearly EW polarizations at MNT occur mostly in the period immediately before the eruption when there are 90°-flips in shear wave polarizations, see Fig. 3(b).

Temporal patterns of the φ parameter for Band-1 arrivals are shown in Fig. 3(b), again using nine-point moving averages in three-point steps. The time pattern at ESP (top panel) shows no significant variations in the analysed period. At MNT (bottom panel), the pattern shows that the qS1 polarization eigendirection flips between 55° and 145° exhibiting two more pronounced variations: the first one approximately at day 90 (∼100 days before July eruption and ∼30 days before the start of the increases in δt in Fig. 3a); the second at about day 185 (2 to 3 days before July 17). In the same panel, we plot for station MNT, the distribution of polarization directions in a rose-diagram for the pre-eruptive seismic swarm between July 12 and 13. The diagram shows 90°-flips with φ almost orthogonal to the main direction obtained for the entire analysed period shown in Fig. 1.

DISCUSSIONS AND CONCLUSIONS

We routinely investigated the dependence of both δt and φ from backazimuth, focal mechanisms and initial polarizations, excluding that the splitting parameters measurements are dependent on this parameters. We measured the time variations of the splitting parameters at Mt Etna before, during, and after the 2001 July effusive eruption. Our observations described in the previous sections show:

(1) At both stations ESP and MNT, Band-1 δt arrivals show similar patterns: a long-term increase that begins several of days before the start of the effusive eruption, and a short-term decrease starting 2 to 3 days before the eruption (Fig. 3a).

(2) At both stations ESP and MNT, φ is aligned in a NNW–SSE direction, apart from EW polarizations at MNT immediately before the eruption (Figs 1 and 3b).

(3) The time pattern of φ variations at Station ESP shows no significant change, while at Station MNT, there are several pronounced 90°-flips, jumping between 55° and 145°. φ begins with a 90°-flip, and there is a brief excursion at day 50, but the major persistent 90°-flips are at day 90 and day 185 (Fig. 3b).

Increasing in time delays

An increase of the average time delay along ray paths in the double-leafed solid angle of directions Band-1 corresponds to an increase in the aspect-ratio of the EDA cracks. Similar increases have been observed before some 15 earthquakes worldwide (Crampin *et al.* 1990, 1991; Gao *et al.* 1998; Volti & Crampin 2003b; Gao & Crampin 2004; Crampin & Gao 2005) and elsewhere). APE modelling suggests (Crampin & Zatsepin 1997; Crampin 1999) that the observed long-term increase of δt is monitoring the effects of the accumulation of stress on modifications to microcrack geometry. The accumulation of stress continues until a level of cracking, referred to as fracture criticality, is reached when the rocks are so fractured that they reach the percolation threshold and the rock fractures (Crampin 1994). Thus the increase in time delays in Fig. 3(a) may be interpreted as monitoring stress accumulation before lava fractures the surface in the eruptive phase. Such 'magma'-fractures are analogous to hydro-fracture operations in the oil industry.

Decreasing time delays

Similarly, decreases in the average δt immediately before the onset of the eruption are also observed immediately before earthquakes (whenever there are sufficient observations immediately before the event to display the phenomenon, Gao & Crampin 2004). These decreases are interpreted as a stress relaxation caused by crack coalescence as the fault plane approaches the onset of fracturing. The observation of an abrupt short-term decrease in δt, 2 to 3 days before the eruption, may be analogous to the decreases in δt observed before earthquakes. This may suggest a similar phenomenon of crack coalescence, leading to stress relaxation, before the eruption.

Values of normalized time delays

The normalized shear wave splitting time delays are less than 8 ms km^{-1} in most crustal rocks (Crampin 1999). Only in Iceland (Volti & Crampin 2003b) and at Mt Vesuvius (Del Pezzo *et al.* 2004) there are time delays reaching the same level as observed in Fig. 3(a). Shear wave splitting is very sensitive to details of crack and pore-fluid geometry; in particular the time delay varies strongly with properties of matrix rocks such as Poisson's ratio, and with properties of the pore-fluid (pressure, acoustic velocity, viscosity, etc.). All these previous properties change with the temperature, consequently the higher values of δt in volcanic areas have been attributed by Crampin (1993) and Volti & Crampin (2003b), to the effects of high heat flow on the response of shear wave splitting to different crack conditions. This may be also the cause of the high δt values at Mt Etna.

Rose-diagrams

The rose-diagrams in Fig. 1 show that at both stations φ is aligned in the same direction and are compatible with the NS direction of the regional stress-field (Patanè *et al.* 2003; Musumeci *et al.* 2004). These observations allow us to interpret the splitting parameters as due to pervasive, approximately NS stress-aligned, fluid-filled microcracks, confirming previous observations at Mt Etna (Bianco *et al.* 1998).

90°-flips in shear wave polarizations

APE modelling suggests that when increasing pore-fluid pressures reach critically high levels (as they do on all seismically active faults), the effective stress-field realigns microcrack distributions, and causes 90°-flips in shear wave polarizations (Crampin *et al.* 2004, and references therein). Extending this interpretation to our current observations, before day 90, the polarizations of φ average about the regional stress direction of about N140°E . The initial flip and the excursion around day 50 are presumably minor variations as stress and pressures change; in particular, the variation at day 50 occurs in coincidence with the opening of a new eruptive fissure in the summit craters area; we did not discuss this point further since we were interested in studying the relationship, if any, between the temporal trend of the splitting parameters and the occurrence of the main effusive eruption. The 90°-flip at day 90, may be the effects of increasing pressure as magma approaches the surface close to Station MNT. This reorganizes the local microcrack geometry and causes 90°-flips in the φ polarizations at MNT. After day 90, the 90°-flip persists at, approximately N50°E polarization (in this period the seismicity does not sample the shallower layers, see Fig. 4), until 5 days before the eruption again shows a 90°- flip, returning to regional stress directions, suddenly followed by another flip that may reflect the effects of pressure/stress relaxation and crack coalescence immediately before the eruption. The ESP station does not show the same time pattern for φ possibly because the overpressure regime is confined to the immediate neighbourhood of the fracture, indicating that the effects of high pressure rapidly decays with distance.

To our knowledge, there are four previous observations of variations in shear wave splitting related to volcanic eruptions. Miller & Savage (2001) and Gerst & Savage (2004) recorded φ variations showing 90°-flips before and after the 1995/1996 eruption at Ruapehu, New Zealand. Bianco *et al.* (1998) observed variations in δt during the propagation of a dry syn-eruptive fracture for the 1989 eruption at Mt Etna, Sicily. Volti & Crampin (2003b) observed increases of δt in Band-1 for about 3 months before the 1996 fissure eruption at Vatnajökull, Iceland (these variations were observed at distances up to 240 km).

The present observations show long- and short-term variations in δt and 90°-flips in φ that are directly similar to those seen before

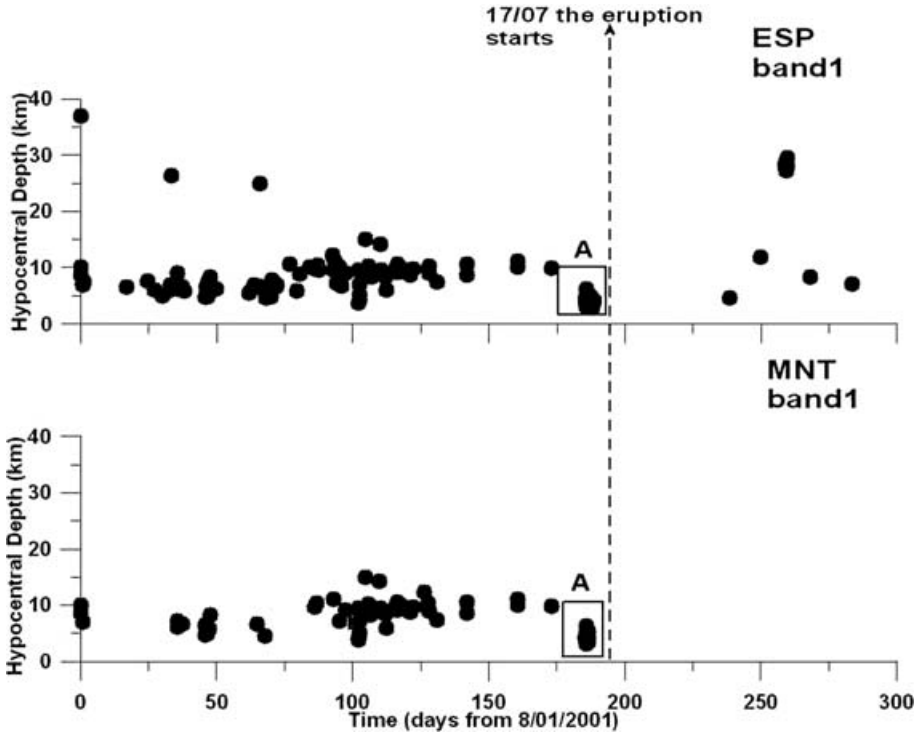

Figure 4. Temporal distribution of the hypocentral distances (straight line) at each station. In the box A the shallower pre-eruptive swarm is reported.

earthquakes, possibly suggesting that the build-up of the stress before fissure eruptions is, in some way, similar to the build-up of stress before earthquakes.

Temporal and spatial variations

Recently a great debate arose on the spatial or temporal origin of an observed coseismic increase in anisotropy time delay for the aftershock zone of the 1999 Chi-Chi (Taiwan) earthquake (Liu *et al.* 2005a,b; Crampin & Gao 2005). In addition, Peng & Ben-Zion (2005) interpreted the changes in anisotropy for the aftershocks of the 1999 Izmit and Duzce (Turkey) sequence, as due mainly to the changing in ray paths, and hence due to spatial variations of the analysed seismicity. In the following paragraphs we discuss the possibility that the measured variation of the splitting parameters at Mt Etna before the occurrence of the 2001 eruption may reflect spatial variations of the analysed seismicity and/or spatial variation of the anisotropic features and not temporal variation of the anisotropy.

As first step we investigate on the possibility that the spatial normalization may account for the measured temporal variation in δt; in other words, since the parameter δt is normalized for the hypocentral distance, the apparent change in δt could be due to change in the depth of earthquakes.

Looking at the temporal distribution of the hypocentral distances (Fig. 4, box A) it may be observed an almost constant pattern, but with an apparent slight decrease just before the occurrence of the eruption. If the observed pattern of δt were produced only by the effect of normalization, we would observe an increase of δt associated with the decrease of the hypocentral distance (being the time delay divided for a smaller hypocentral distance). However, the events in box A of Fig. 4, occurring 2 to 3 d before the eruption, show, on the contrary, an anticorrelated pattern (a sudden decrease, Fig. 3a). This evidence, in our opinion, may suggest that the observed pattern for δt is not due to the normalization of δt to the hypocentral distance.

To further investigate on the effect of any space variations in the temporal trend of δt and φ, we depict the volume sampled by the ray paths relative to the earthquakes utilized.

We use a parabolic ray tracing based on the 3-D tomographic velocity model of Etna (Patanè *et al.* 2002), plotting the parabolas in the vertical plane connecting source and station that represent the Fermat's path of minimum traveltime. In Fig. 5 the WE and NS projections of the rays relative to the seismicity occurred until 2001 July 11 are plotted in blue, while the rays of the seismicity occurred after this date (until the eruption starts for ESP, and until July 13 for MNT) are in plotted in red. In both periods the rays, under each station, seem to laterally sample the same crustal extent, even though with different depths; in addition, a spatial superposition of the shallower rays with the deeper ones is also observed.

We observe the temporal variation of δt in the sole Band-1; at MNT station the mean value of incidence (Von Mises statistic) is $25^\circ \pm 3^\circ$, at ESP station is $30^\circ \pm 2^\circ$; this evidence indicates that the rays span a volume that is poorly extended laterally, as shown in Fig. 5, where only Band-1 is reported. To fix the ideas we image the anisotropic volume [responsible for the observed variation of the splitting parameters] as a sort of ray tube, approximately spanning the first 8–10 km from the topographical surface under each station, with a maximum lateral extension of 1.5 km (see Fig. 5). Due to the narrowness of this tube, it is unlikely that the anisotropic features change spatially so much to give the pattern for δt reported in Fig. 3(a), even though in principle we cannot rule out this hypothesis. We favour the hypothesis of temporal change taking also into account the observation that the trend of δt in time is the same at

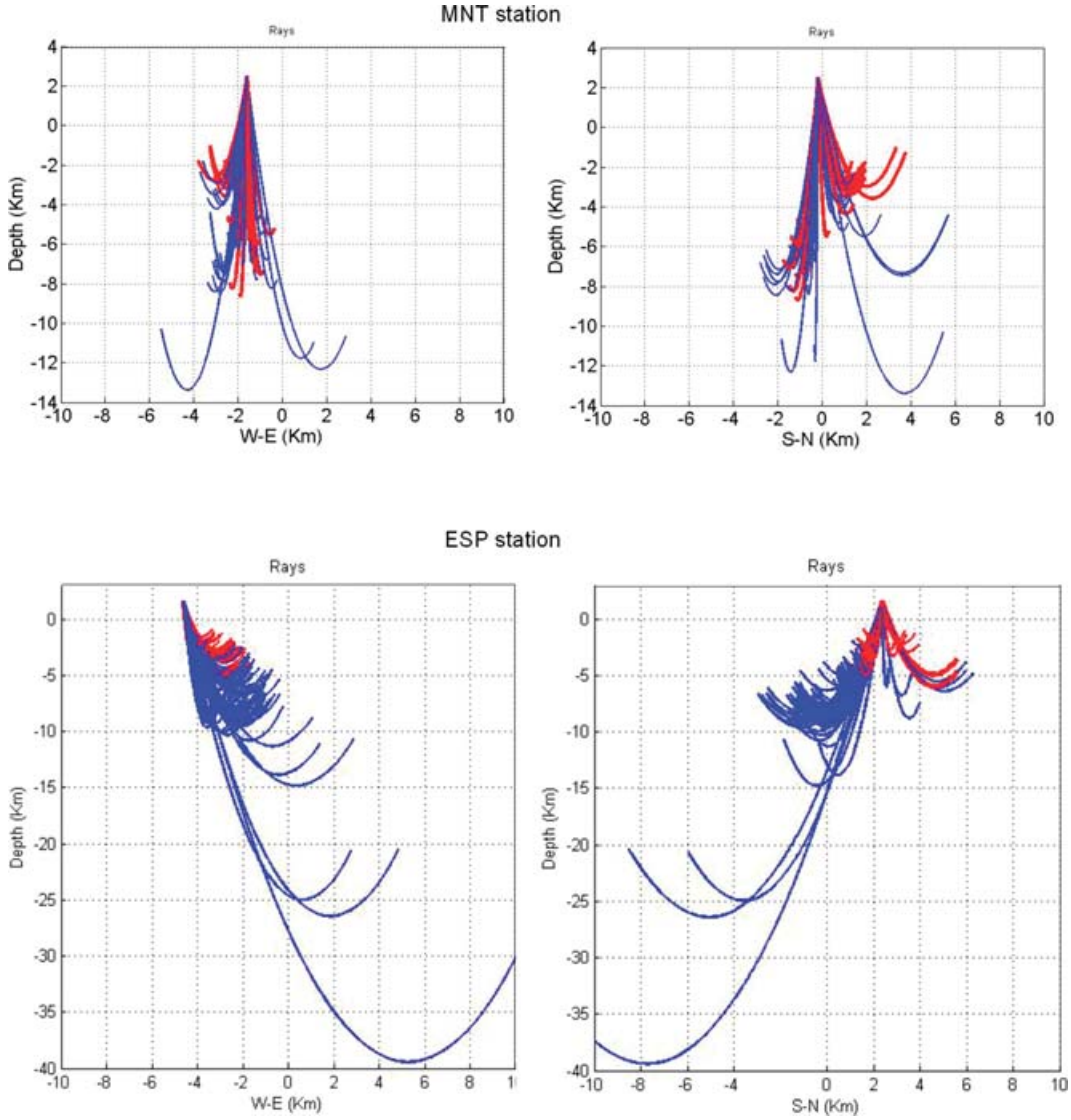

Figure 5. Rays coverage for the sampled anisotropic volume at MNT and ESP stations. The WE and NS projections of the rays relative to the seismicity occurred until 2001 July 11 are plotted in blue, while the rays of the seismicity occurred after this date (until the eruption starts for ESP, and until July 13 for MNT) are in red.

both stations (see Fig. 3a) and that φ exhibits the same main direction at both stations (see Fig. 1); we are confident enough that the overall seismicity sample the same pervasive fluid-aligned vertical cracks under both stations.

An alternative explanation to our observations may be the following: the shallow earthquake swarms, occurring just before the eruption starts, led to preferential sampling of shallow crustal regions with anisotropic features different from the volume that the deepest seismicity sampled. In other words, the shallower layer (the first 5 km b.s.l.?) is characterized by cracks closer than those in the deeper layer (5–10 km b.s.l.) that poorly affect the shear wave propagation. Going in more details, observing that φ for the shallower pre-eruptive seismicity is oriented orthogonal to φ for the deeper seismicity, the shallow anisotropic volume may be characterized by fluid-filled cracks oriented at 90° with respect the orientation of the cracks sampled by the deeper seismicity.

The present analysis is not carried out using doublets (no doublets in our data set), and this in principle does not exclude that the observed changes reflect space changes of the sources and not temporal changes in the anisotropic features of the medium. However, in our data set we found two events occurred at the end of 2001 February and on July 13 (during the pre-eruptive swarms), with the same source depth and a lateral separation of 0.5 km. These events exhibit δt (the non-normalized value of the time lag between qS1 and qS2) equal to 0.05 s for the first and 0.12 s for the second event; $\varphi = 155^\circ$ for the first and $\varphi = 67^\circ$ for the second event. It is reasonable that the rays of these two events sampled approximately the same volume, so that this observation may favour the interpretation of a temporal and not of a spatial variation of the crustal seismic anisotropy associated with the 2001 volcanic eruption at Mt Etna. The alternative hypothesis seems unreasonable as it would imply that the anisotropic features strongly vary within the small distance of 0.5 km.

However, we are aware that the characteristics of the analysed data set do not allow to definitively choose among the two different interpretations presented in this paper; but we favour the hypothesis

that the observed changes of the splitting parameters may be interpreted in terms of changes in the stress field acting in the area, in turn producing changes in the aspect ratio of the cracks according to the following considerations/observations:

(i) The normalization of the time delay to the hypocentral distance seems not to be responsible for the observed temporal pattern of δt, as discussed previously.

(ii) The volume sampled by the analysed seismicity has small lateral extent and does not laterally change when the pattern of δt shows the most significant variations (at both stations)

(iii) δt behaviour shows the same pattern at both stations

(iv) the splitting parameters time behaviour exhibits the same trend observed elsewhere before the occurrence of several earthquakes worldwide.

Future analysis performed on doublets may give more constraints on the interpretation of the pattern observed for the splitting parameters at Mt Etna, possibly clarifying definitively if these parameters temporally change with the occurrence of the main eruptive episodes.

ACKNOWLEDGMENTS

We thank the editor Thorsten Becker for the careful reviews and the useful suggestions; we also thank Alexander Druzhinin and an anonymous reviewer for their comments and criticisms; Stuart Crampin is thanked for insightful comments and suggestions. This work was funded by the Italian Dipartimento della Protezione Civile in the frame of the 2004–2006 Agreement with Istituto Nazionale di Geofisica e Vulcanologia—INGV (Project V4) and by the European Union VOLUME FP6-2004-GLOBAL-3.

REFERENCES

Bianco, F., Castellano, M. & Ventura, G., 1998. Structural and seismological features of the 1989 syn-eruptive NNW-SSE fracture system at Mt. Etna, *Geophys. Res. Lett.,* **25,** 1545–1548.

Bokelmann, G.H.R. & Harjes, H.-P., 2000. Evidence for temporal variation of seismic velocity within the upper continental crust, *J. geophys. Res.,* **105,** 23 879–23 894.

Born, M. & Wolf, E., 1965. *Principles of optics,* 3rd edn, Pergamon Press, New York.

Crampin, S., 1981. A review of wave motion in anisotropic and cracked elastic-media, *Wave Motion,* **3,** 343–391.

Crampin, S., 1993. A review of the effects of crack geometry on wave propagation through aligned cracks, *Can. J. Expl. Geophys.,* **29,** 3–17.

Crampin, S., 1994. The fracture criticality of crustal rocks, *Geophys. J. Int.,* **118,** 428–438.

Crampin, S., 1999. Calculable fluid-rock interactions, *J. Geol. Soc.,* **156,** 501–512.

Crampin, S. & Chastin, S., 2003. A review of shear-wave splitting in the crack-critical crust, *Geophys. J. Int.,* **155,** 221–240.

Crampin, S. & Zatsepin, S.V., 1997. Modelling the compliance of crustal rock-II. Response to temporal changes before earthquakes, *Geophys. J. Int.,* **129,** 495–506.

Crampin, S. & Gao, Y., 2005. Comment of on 'Systematic analysis of shear-wave splitting in the aftershock zone of the 1999 Chi-Chi earthquake: shallow crustal anisotropy and lack of precursory variations', by Liu, Y., Teng, T.-L. & Ben Zion, Y., *Bull. Seism. Soc. Am.,* **95,** 354–360, doi:10.1785/0120040092.

Crampin, S., Evans, R. & Atkinson, B.K., 1984. Earthquake prediction: a new physical basis, *Geophys. J. R. astr. Soc.,* **76,** 147–156.

Crampin, S., Booth, D.C., Evans, R., Peacock, S. & Fletcher, J.B., 1990. Changes in shear wave splitting at Anza near the time of the North Palm Springs Earthquake, *J. geophys. Res.,* **95,** 11 197–11 212.

Crampin, S., Booth, D.C., Evans, R., Peacock, S. & Fletcher, J.B., 1991. Comment on 'Quantitative Measurements of Shear Wave Polarisations at the Anza Seismic Network, Southern California: implications for Shear Wave Splitting and Earthquake Prediction' by Aster, R.C., Shearer, P.M. & Berger, J., *J. geophys. Res.,* **96,** 6403–6414.

Crampin, S., Volti, T. & Stefansson, R., 1999. A successfully stress-forecast earthquake, *Geophys. J. Int.,* **138,** F1–F5.

Crampin, S., Volti, T., Chastin, S., Gudmundsson, A. & Stefánsson, R., 2002. Indication of high pore-fluid pressures in a seismically-active fault zone, *Geophys. J. Int.,* **151,** F1–F5.

Crampin, S., Peacock, S., Gao, Y. & Chastin, S., 2004. The scatter of time-delays in shear-wave splitting above small earthquakes, *Geophys. J. Int.,* **156,** 39–44.

Del Pezzo, E., Bianco, F., Petrosino, S. & Saccorotti, G., 2004. Changes in the coda decay rate and shear wave splitting parameters associated to seismic swarms at Mt. Vesuvius, Italy, *Bull. seism. Soc. Am.,* **94,** 439–452.

Gao, Y. & Crampin, S., 2004. Observations of stress relaxation before earthquakes, *Geophys. J. Int.,* **157,** 578–582.

Gao, Y., Wang, P., Zheng, S., Wang, M., Chen, Y.-T. & Zhou, H., 1998. Temporal changes in shear-wave splitting at an isolated swarm of small earthquakes in 1992 near Dongfang, Hainan Island, southern China, *Geophys. J. Int.,* **135,** 102–112.

Gerst, A. & Savage, M.K., 2004. Seismic anisotropy beneath Ruapehu Volcano; a possibile eruption forecasting tool. *Science,* **306,** 1543–1547.

Li, Y.-G., Teng, T.L. & Henyey, T.L., 1994. Shear-wave splitting observations in the northern Los Angeles Basin, Southern California, *Bull. seism. Soc. Am.,* **84,** 307–323.

Liu, Y., Crampin, S. & Main, I., 1997. Shear-wave anisotropy: spatial and temporal variations in time-delays at Parkfield, Central California, *Geophys. J. Int.,* **130,** 771–785.

Liu, Y., Teng, T.L. & Ben-Zion, Y., 2004. Systematic analysis of shear wave splitting in the aftershock zone of the 1999 Chi-Chi, Taiwan, earthquake: shallow crustal anisotropy and lack of precursory variation, *Bull. seism. Soc. Am.,* **94,** 2330–2347.

Liu, Y., Teng, T.-L. & Ben Zion, Y., 2005a. Systematic analysis of shear-wave splitting in the aftershock zone of the 1999 Chi-Chi earthquake: shallow crustal anisotropy and lack of precursory variations, *Bull. seism. Soc. Am.,* **94,** 2330–2347.

Liu, Y., Teng, T.-L. & Ben Zion, Y., 2005b. Reply to Comment of Crampin and Gao on 'Systematic analysis of shear-wave splitting in the aftershock zone of the 1999 Chi-Chi earthquake: shallow crustal anisotropy and lack of precursory variations', by Liu, Y., Teng, T.-L. & Ben Zion, Y., *Bull. Seism. Soc. Am.,* **95,** 361–366, doi:10.1785/0120040109.

Miller, V. & Savage, M., 2001, Changes in seismic anisotropy after volcanic eruptions: evidence from Mt. Ruapehu, *Science,* **293,** 2231–2233.

Musumeci, C., Cocina, O., De Gori, P. & Patanè, D., 2004. Seismological evidence of stress induced by dike injection during the 2001 Mt. Etna eruption, *Geophys. Res. Lett.,* **31,** L07617, doi:10.1029/2003GL019367.

Patanè, D., Chiarabba, C., Cocina, O., De Gori, P., Moretti, M. & Boschi, E., 2002. Tomographic images and 3D earthquake locations of the seismic swarm preceding the 2001 Mt. Etna eruption: evidence for a dyke intrusion, *Geophys. Res. Lett.,* **29**(10): doi:10.1029/2001GL014391.

Patanè, D., De Gori, P., Chiarabba, C. & Bonaccorso A., 2003. Magma ascent and the pressurization of Mount Etna's volcanic system, *Science,* **299,** 2061–2063.

Peacock, S., Crampin, S., Booth, D.C. & Fletcher J.B., 1988. Shear wave splitting in the Anza seismic gap, Southern California: temporal variations as possible precursors, *J. geophys. Res.,* **93,** 3339–3356.

Peng, Z. & Ben-Zion, Y., 2005. Spatio-temporal variations of crustal anisotropy from similar events in aftershocks of the 1999 M7.4 Izmit and M7.1 Duzce, Turkey, earthquake sequences, *Geophys. J. Int.,* **160,** 1027–1043.

Shieh, C.F., 1997. Estimation of shear-wave splitting time using orthogonal transformation, *Geophysics,* **62,** 657–661.

Tang, C., Rial, J.A. & Lees, J.M., 2005. Shear-wave splitting: A diagnostic tool to monitor fluid pressure in geothermal fields, *Geophys. Res. Lett.,* **32,** L21317, doi:10.1029/2005GL023551.

Teanby, N., Kendall, J.M., Jones, R.H. & Barkved, O., 2004. Stress-induced temporal variations in seismic anisotropy observed in microseismic data, *Geophys. J. Int.,* **156,** 459–466.

Volti, T. & Crampin, S., 2003a. A four-year study of shear-wave splitting in Iceland: 1. Background and preliminary analysis, in *New insights into structural interpretation and modelling,* Vol. 212, pp. 117–133, ed. Nieuwland, D.A., Geol. Soc. Lond., Spec. Publ.

Volti, T. & Crampin, S., 2003b. A four-year study of shear-wave splitting in Iceland: 2. Temporal changes before earthquakes and volcanic eruptions, in *New insights into structural interpretation and modelling,* Vol. 212, pp. 135–149, ed. Nieuwland, D.A., Geol. Soc. Lond., Spec. Publ.

Zatsepin, S.V. & Crampin, S., 1997. Modelling the compliance of crustal rock: I - response of shear-wave splitting to differential stress, *Geophys. J. Int.,* **129,** 477–494.